U.S. Department of Commerce
National Oceanic and Atmospheric Administration
National Weather Service
National Centers for Environmental Prediction
5830 University Research Court
College Park, MD 20740-3818

Office Note 486

http://dx.doi.org/10.7289/V5/ON-NCEP-486

A MINOR MODIFICATION OF THE GNOMONIC CUBED-SPHERE GRID THAT OFFERS ADVANTAGES IN THE CONTEXT OF IMPLEMENTING MOVING HURRICANE NESTS

R. James Purser * and Mingjing Tong
IM Systems Group, Rockville, Maryland

June 13, 2017

* email: jim.purser@noaa.gov

Abstract

The next generation of operational weather and climate prediction models of the National Weather Service is planned to comprise versions of the GFDL FiniteVolume Cubed-Sphere Dynamical Core (FV3). In order to address the need to accommodate storm-tracking movable nests during seasons when tropical storms are active, we will be confronted with cases where the nested grid must pass over the corners of the cubed sphere grid, which are situated at approximately 35° of latitude. Although this latitude is already sufficiently large to make such a passage relatively rare, and although there is no doubt that the technical challenge of achieving a smoothly-progressing nest in such a situation will be (indeed, must be) met, a very small modification to the parent grid, from purely cubic to prolate prismatic, might be an attractive way to make these occurrences even less frequent. This note presents what seems to be an elegant way that such a minor modification of the grid might be made without changing two of its characteristic features: the grid lines will all remain great circles on the sphere; and the grid cells at the centers of each of the six 'tiles' will remain square. The equiangular distribution of those of the grid lines of the equator-straddling tiles that correspond to lines of constant longitude is also preserved (the other families of grid lines are no longer perfectly uniformly spaced in angle). But by nudging the latitudes of the tile corners poleward by even a very small angle we will fairly dramatically further reduce the frequency at which storm-tracking nests will need to interact with these corners of the parent grid.

1. Introduction

The cubed-sphere grid geometry, based on gnomonic projections to each of the six faces or 'tiles' was first proposed as a framework for global numerical weather simulation by Sadourny (1972). Much later, as we began to enter the modern era of massively parallel computing, the idea was independently reconsidered simultaneously by, for example, Ronchi et al. (1996), Rančić et al. (1996), and McGregor (1996, 1997), as a natural solution to the need to avoid unnecessary global communications (such as in the Fourier filtering needed at high latitudes of the longitude and latitude grid framework) if high computational efficiency and scalability were to be guaranteed in the new computing paradigm.

As the results of comparisons made in the course of the competition amongst models participating in the Next Generation Global Prediction System (NGGPS) project, the one chosen for development as the future operational global model at NCEP was the GFDL's 'FV3' finite-volume model, a direct descendant of the model formulated by Lin and Rood (1996), Lin (2004) and reconfigured to an equiangular variant of the gnomonic grid framework by Putman and Lin (2007). Among the attractive geometrical features of this grid framework, as recognized by Sadourny, is its inherent simplicity, and the fact that all of the grid lines are great-circles of the sphere, so that grid-curvature issues never have to be faced. The edges and corners of the cube, while certainly singularities (in a trivial sense) of the grid, are *not* singularities of the underlying coordinates of each tile's grid. Therefore, it is not too difficult to accurately accomplish the interpolations necessary to enable solutions on either side of an edge, or on the three sectors around a corner, to properly match, whether this is done in a global model or on a moveable nest. Nevertheless, when it comes to presenting the moveable nested grids that we need in order to track tropical storms, the edges of the nest will 'kink' wherever they cross an edge of the cube. While, with a fixed global parent grid, it is almost inevitable that hurricane nests will frequently be required to traverse the edges of the cube, it would certainly be desirable not to have to encounter the even more awkward corner regions of the grid (at about 35° of latitude in the cube, as shown in Fig. 1) any more than is absolutely necessary. In fact, it might be worth considering a minor modification to the definition of the grid framework, since a very small nudging poleward of the locations of these corners would most likely reduce, by quite a dramatic degree, the frequency of such encounters with a mobile storm-tracking nest.

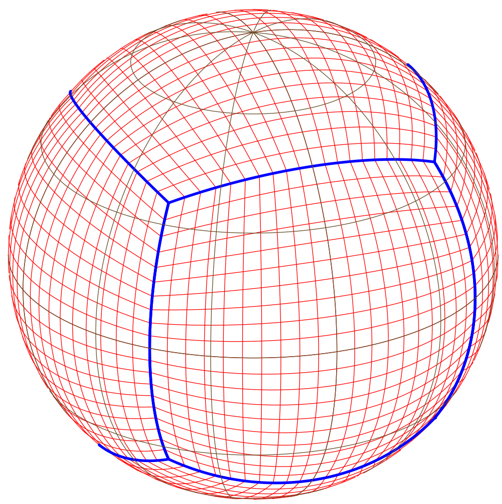

Figure 1. The equiangular gnomonic cubed sphere grid with conventional geographical coordinate lines shown every 30°. The corners of the cubic grid occur at around latitudes $\pm 35.26^\circ$.

This note explores a very simple and systematic modification to the equiangular modification of the gnomonic cubed-sphere grid which corresponds to a grid geometry that is no longer purely cubic, but is instead derived from the geometry of a slightly prolate (elongated) square (in cross-section) prism. The grid domains of the two end faces, or polar tiles, of this geometry remain perfectly square (although reduced in effective area) while the grids of the four equator-straddling 'side tiles' become rectangles elongated in the meridional dimension, rather than squares, and are thereby slightly increased in size when the number of longitude grid lines is kept constant. The proposed modification is designed to preserve the characteristic feature that the grid lines remain great-circles. We also show that this can be accomplished in such a way that the density of spacing of grid lines in each family remains continuous across the edges of this new cuboid, just as it was on the original cubed sphere, and, for the family of longitude grid lines of the side tiles, these lines can also preserve the equiangular spacing property. The proposed new configuration is obviously slightly less symmetric and would therefore entail a slightly more general handling of some of the numerics. The grid lines on the polar tiles can no longer be equally spaced in angles, and neither can the quasi-zonal grid lines of the side tiles. Also, the edges meeting at the eight corners can no longer do so at equal 120° angles; the angle becomes a little larger at the side tile corners and compensatingly smaller at the corner of the polar tile. In other respects, the simplicity of the geometrical configuration of the grid is largely preserved.

2. Constructing a prolate prism grid with great circles

The distribution of one family of grid lines on the polar tile can be conveniently parameterized by the longitude, θ, relative to that of the median grid line of this family, at which this grid line intersects the edge of the tile. Since we want each grid line to meet its longitude-line counterpart in the equator-straddling 'side tile' on the other side of that edge, we cannot generally keep the angular distribution of these matched families of grid lines uniform in both the polar tile and the side tile when the cube is replaced by a prolate square prism in the projective definitions of the tile edges. But we can at least keep the angular density of the longitude lines in the side tiles uniform, which is a natural choice. In which case, it is also natural to adopt the (relative) longitude of the side tile grid lines as an informative label, or 'index parameter' attached to the matching family of lines that cover the neighboring polar tile. Each such family clearly has index parameter θ extending within the range, $[-\pi/4, \pi/4]$ with the associated grid lines marked off at uniform intervals of the index parameter. But the natural measure of the angular distribution of the lines in the polar tile is not this index variable, θ, but rather it is the colatitude (as well as the negative of this, to ensure smooth continuity across the entire tile), which we shall call β, of the midpoint of each grid line there. Only for the special case of an exact cube does $\beta(\theta) = \theta$; more generally, in the case of a prolate square prism whose polar-tile edge-midpoints have a colatitude $\alpha < \pi/4$, we will find that $\beta \neq \theta$ (except at the central grid line passing through the pole itself). The relationship is simply:

$$\tan(\theta)\tan(\alpha) = \tan(\beta). \tag{2.1}$$

Fig. 2 shows the geometry of the various angles and parameters in our notation.

Although the family of polar tile grid lines parameterized by θ and located by their midpoint colatitudes, β goes only as far as the tile edge, $\beta = \alpha$, the family can be analytically extrapolated beyond that edge into the neighboring side-tile, whereupon the same lines, getting now progressively longer as we approach the equator, $\beta = \pi/2$, describe the roughly east-west aligned grid lines of this side panel. But the label, θ, implied by (2.1), which is used in the polar panel as an index-parameter does not adequately serve that purpose in the side panel if we want the density of grid lines to diminish monotonically as they approach the equator and to attain the same density of the longitude grid lines there (to ensure that grid cells become square at the equatorial centers of these side tiles). Fig. 3a shows the nonlinear distribution of θ plotted against β from pole ($\beta = \theta = 0$ to equator ($\beta = \theta = 90°$) in the illustrative example of extreme prolateness, $\alpha = 30°$; Fig. 3b shows the density of the index parameter with respect to the colatitude β of line-midpoints as a solid curve in the polar tile, and its analytic extension continuing as the dashed curve into the side tile, where it exhibits an undesirably low implied resolution. A more desirible form for this density in the side tile is shown by the blue curve, smoothly preserving the rate of change of density at the transition point, $\beta = \alpha$, but curving to a desirable value of unity at the equator. We rename the index parameter of the east-west aligned grid lines of the side tile, $\hat{\theta}$, setting its value to zero at the equator, and replacing

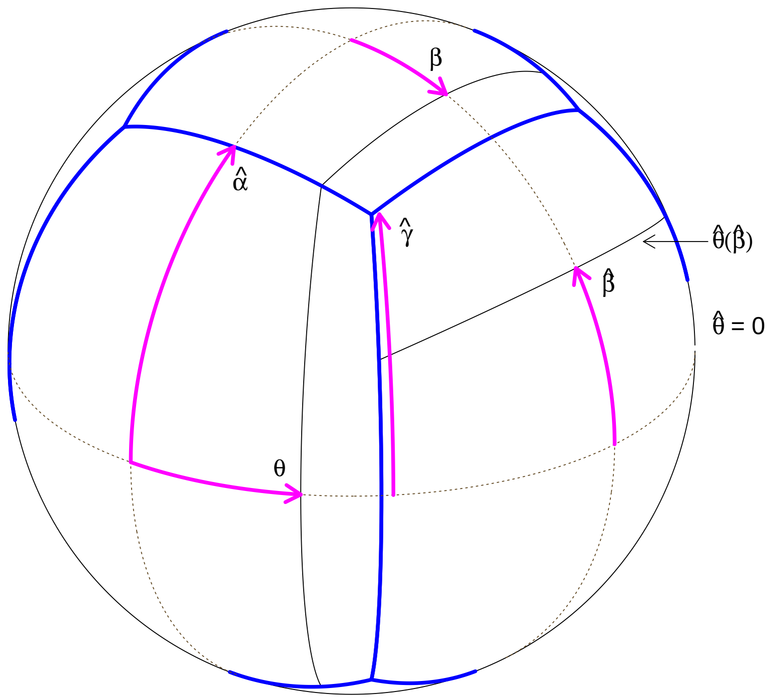

Figure 2. Schematic description of angles and parameters defined for the geometry of the prolate prism grid.

the midpoint colatitudes β and α by the equivalent latitudes, $\hat{\beta} = \pi/2 - \beta$ and $\hat{\alpha} = \pi/2 - \alpha$, to simplify some of the algebraic expression. To achieve the desired degree of continuity, we match the first and second derivatives of $\theta(\beta)$ with the first derivative, and the negative of the second derivative, of $\hat{\theta}(\hat{\beta})$ at tile edge, $\beta = \alpha$.

It is first helpful to define the function,

$$q(\beta) = \frac{1}{\tan^2(\alpha)\cos^2(\beta) + \sin^2(\beta)} = \frac{1}{1 - (1 - \tan^2(\alpha))\cos^2(\beta)}. \tag{2.2}$$

so that the profile of $\hat{\theta}$ and its derivatives as a function of β can be set out for the polar tile as follows.

$$\hat{\theta}(\beta) = \arctan(\tan(\beta)/\tan(\alpha)), \tag{2.3}$$

$$\frac{d\hat{\theta}(\beta)}{d\beta} = q(\beta)\tan(\alpha), \tag{2.4}$$

$$\frac{d^2\hat{\theta}(\beta)}{d\beta^2} = -2q^2(\beta)\tan(\alpha)\cos(\beta)\sin(\beta)(1 - \tan^2(\alpha)). \tag{2.5}$$

We denote the excess density of lines at this edge by h, defined by:

$$1 + h = \frac{d\theta(\alpha)}{d\beta} \equiv \frac{d\hat{\theta}(\hat{\alpha})}{d\hat{\beta}} = \frac{1}{\sin(2\alpha)}, \tag{2.6}$$

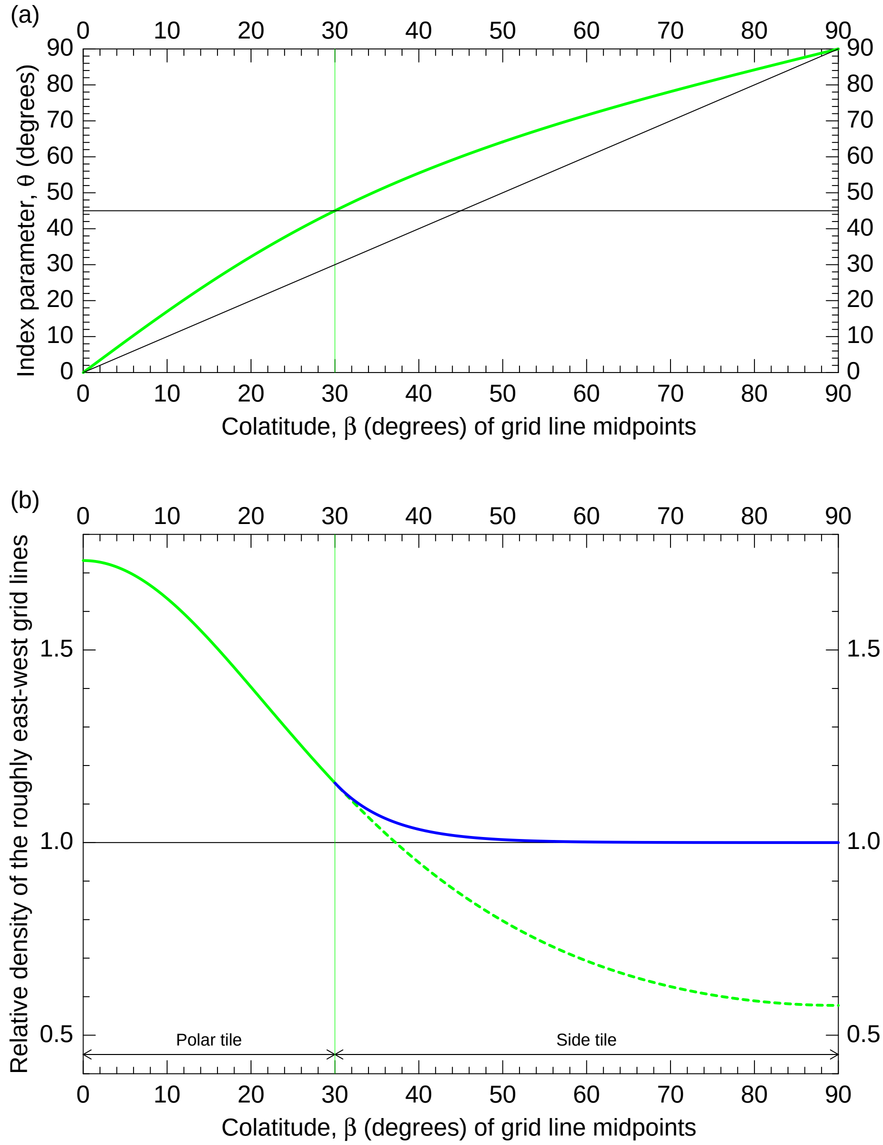

Figure 3. For a rather extreme choice of the prolateness angle parameter, $\alpha = 30^\circ$, panel (a) shows how the index parameter, θ, as a function of the colatitude, β, of the midpoints of quasi-zonal grid lines, is in generally steeper than unity in the polar tile, $\beta < \alpha$ but becomes relatively shallower in slope when extrapolated into the side tile. The thin black diagonal line shows the case of the unaltered cube for comparison. The density of grid lines (i.e., the derivative of the index parameter) is shown more clearly in panel (b), dashed in the extrapolated region. In order to fit a series of quasi-zonal grid lines in the side panel ($\beta > 30^\circ$, in this case) without their density dropping below unity, we need an adjusted profile of the density like that shown by the solid blue curve, which matches both the polar tile's line density and the derivative of it, at the tile edge, $\beta = \alpha$.

and the rate of change of this density of lines across the edge (in the poleward direction) by,

$$g = -\frac{d^2\theta(\alpha)}{d\beta^2} \equiv \frac{d^2\hat{\theta}(\hat{\alpha})}{d\hat{\beta}^2} = \frac{2\cos(2\alpha)}{\sin^2(2\alpha)}. \tag{2.7}$$

In the interior of the side tile, $\hat{\beta} < \hat{\alpha}$, we assume the excess density, $d\hat{\theta}/d\hat{\beta} - 1$, to take a 'meniscus', 'tensioned spline' (Schweikert, 1966) or flattened catenary shape, rising smoothly from zero at the equator, $\hat{\beta} = 0$, to the matching conditions (2.6) and (2.7) at the poleward tile edge, $\hat{\beta} = \hat{\alpha}$. For a suitably chosen constant, ϕ, this general form is:

$$\frac{d\hat{\theta}}{d\hat{\beta}} = 1 + h\frac{\sinh^2(\phi\hat{\beta}/\hat{\alpha})}{\sinh^2(\phi)}. \tag{2.8}$$

Then, since,

$$\frac{d^2\hat{\theta}}{d\hat{\beta}^2} = \frac{2h\phi \sinh(\phi\hat{\beta}/\hat{\alpha}) \cosh(\phi\hat{\beta}/\hat{\alpha})}{\hat{\alpha} \sinh^2(\phi)}, \tag{2.9}$$

implies,

$$g = \frac{2h\phi}{\hat{\alpha} \tanh(\phi)}, \tag{2.10}$$

we can find the necessary value of ϕ by defining a function $\Phi(z) > 0$ implicitly such that $z = \tanh(\Phi)/\Phi$, whereupon, if we define

$$z = \frac{2h}{g\hat{\alpha}}, \tag{2.11}$$

the constant ϕ we need is obtained as:

$$\phi = \Phi(z). \tag{2.12}$$

(Evaluating the implicit function $\Phi(z)$ numerically for the valid range, $0 < z < 1$, is guaranteed and rapid using the standard Newton-Raphson method, when any moderate first guess, say $\Phi_0 = 1$, launches the convergent iterative evaluations of the reciprocal function, $1/z$, since this function is monotonic, convex and has finitely-bounded derivatives.)

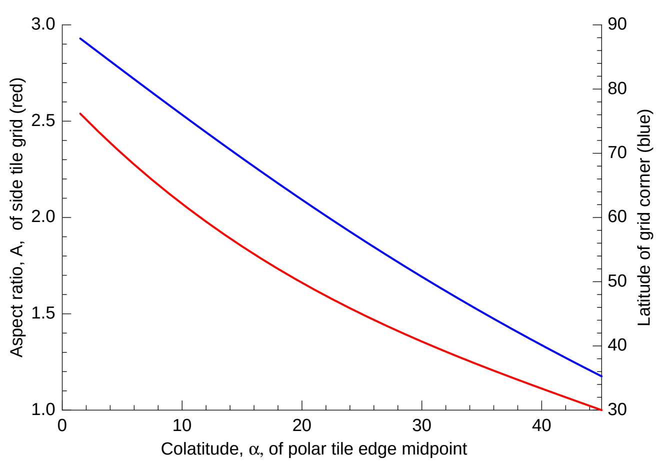

Figure 4. Graphs of side-tile aspect ratio (red curve) and corner latitude (blue curve) as a function of α, the colatitude of the midpoint of the edge of each polar tile.

Evaluating $\hat{\theta}(\hat{\beta})$ simply requires the integration of (2.8), assuming $\hat{\theta}(0) = 0$ for its equatorial value:

$$\hat{\theta}(\hat{\beta}) = \hat{\beta}\left(1 - \frac{h}{2\sinh^2(\phi)}\right) + \frac{h\hat{\alpha}\sinh(\phi\hat{\beta}/\hat{\alpha})\cosh(\phi\hat{\beta}/\hat{\alpha})}{2\phi\sinh^2(\phi)}. \tag{2.13}$$

Since the longitudinal grid spacing around the equator, $\Delta s = \pi/(2N)$, is intended also to serve as the latitudinal grid spacing at the center of the side tile, the condition that an integral number, M, of grid spaces span the meridional extent of the side tile,

$$\hat{\theta}(\hat{\alpha}) = \frac{\pi M}{4N} \equiv \frac{\pi}{4} A(\hat{\alpha}), \tag{2.14}$$

can be satisfied by iteratively seeking the appropriate α, and hence $\hat{\alpha}$, once the suitable degree of prolateness of the side tiles is chosen via the selected ratio, $M : N$ with $M > N$.

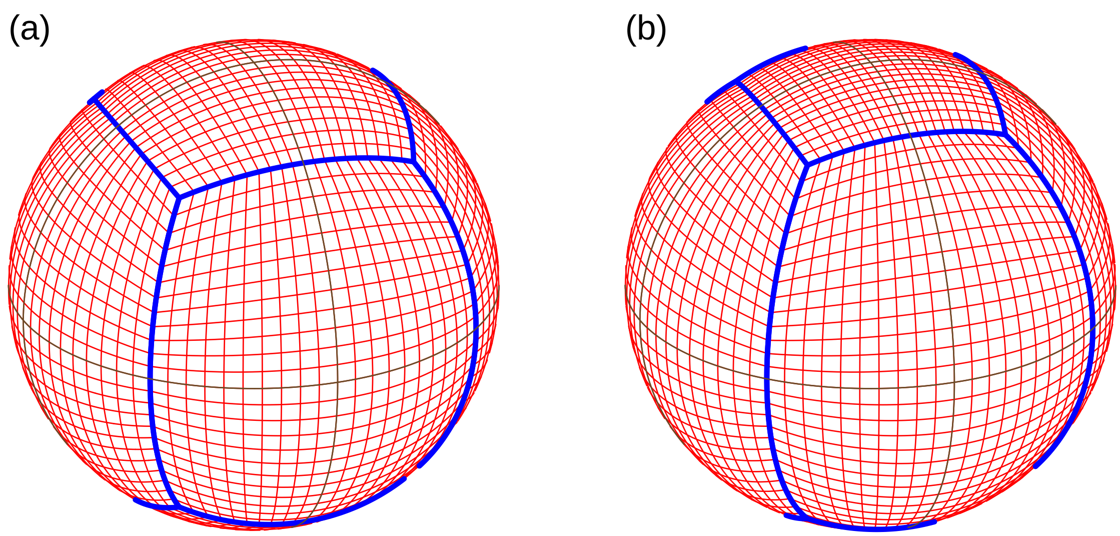

Figure 5. The schematic examples of prolate prism modified gnomonic projection grids. (a) A grid with prolateness angle parameter $\alpha = 36.2^\circ$, which gives side panels with an aspect ratio of $6:5$ and latitude $\hat{\gamma} = 44.0^\circ$ for the grid corners. (b) A grid with prolateness angle, $\alpha = 28.4^\circ$, which gives side panels with an aspect ratio of $7:5$ and latitude $\hat{\gamma} = 52.6^\circ$ for the corners.

The motivation behind this whole exercise is to enable the corners of the grid to have their shared latitude, $\hat{\gamma}$, displaced poleward sufficiently to ensure that dynamically still active tropical cyclones requiring the special scrutiny of a dedicated nested grid much more rarely attain this latitude. Then at least the awkward presentation of an embedded nest passing over the corner of the parent grid is, we expect, avoided in all except a tiny minority of synoptically unusual events. Taking this corner latitude as a function of the prolateness colatitude parameter, α, and using the relationship:

$$\hat{\gamma}(\hat{\alpha}) = \pi/2 - \arctan(\sqrt{2}\tan(\alpha)), \tag{2.15}$$

we can seek the prolateness parameter, α, that is just small enough to render the occurrences of nest-tracked tropical storms reaching the latitude of the corners acceptably rare. Then we can finesse this α so that the aspect ratio,

$$A(\alpha) = \frac{M}{N}, \tag{2.16}$$

is one of the rational values that lets us construct a complete grid on each side tile. (A procrustean alternative, of forcing the M grid spaces to *define* the meridional density of the quasi-zonal lines filling some given side tile shape, would in general fail to satisfy either of the two desiderata: the central grid cells of the side tile would not be square; and the continuity of grid line density passing across the edge with the polar tile would be broken.)

Plotted as functions of the prolateness angle α Fig. 4 shows the corresponding aspect ratio, $A(\alpha)$, and the corner latitude, $\hat{\gamma}(\alpha)$. In Table 1 we plot the estimated percentages of tropical cyclones that, over the last few seasons, have reached the given latitudes. It is striking how quickly the percentages reaching the higher latitudes diminish. Thus, a relatively modest nudging of the corner latitudes in the prism grid will go a long way towards reducing the frequencies of corner-encounters by tropical cyclones. In Fig. 5 we show, using the same perspective as the cube of Fig. 1, two schematic examples of prolate prism grids. Panel (a) shows the degree of prolateness required for an aspect ratio in the side tiles of $6:5$, where the corner latitude becomes $\hat{\gamma} = 44.0°$. Panel (b) shows a more extreme example with an aspect ratio of the side tiles of $7:5$ and corner latitude $\hat{\gamma} = 52.6°$.

3. Generalizations

In principle, it is not necessary to treat both hemispheres equally. The prolateness parameter, α, essentially dictates the sizes of both the polar tiles equally, but these could actually be specified separately with a northern parameter, α_N and a southern parameter, α_S, for example. The distribution of the quasi-zonal grid lines on the side tiles could still be obtained from a tensioned spline matched to the separate excesses of line densities, h_N and h_S, and the rates of change of these densities, g_N and g_S with respect to the $\hat{\theta}$ parameter at the northern and southern polar tile edges. But in this case, the condition required to fix the degree of 'tension' in the spline is not that the excess line density vanish at the equator, but that it vanishes at whatever latitude corresponds to its minimum (an implicit definition, since the location of the minimum must depend upon the tension itself). Probably the only case of this asymmetrical type that could have any practical value would be the special case where the prolateness angle for one hemisphere, say α_S is not changed from the standard, $\alpha_S = \pi/4$, that corresponds to the original cubic configuration. In this case, the spline has its minimum at this same location, since then $h_S = 0$ and $g_S = 0$. Thus, the only algebraic modifications we would need to make in the analysis of the previous section entails replacing $\hat{\alpha}$ and $\hat{\beta}$ by $\tilde{\alpha}$ and $\tilde{\beta}$ in (2.8), (2.9), (2.10), (2.11) and (2.13), where,

$$\tilde{\alpha} = \hat{\alpha} + \pi/4, \tag{3.1a}$$
$$\tilde{\beta} = \hat{\beta} + \pi/4. \tag{3.1b}$$

The newly defined index variable, $\hat{\theta}$, in this case starts at zero at the southern edge of this latitudinally-asymmetrical side tile, rather than in its center, but in other respects, the formalism is very similar.

TABLE 1. THE ESTIMATION OF THE NUMBER/PERCENTAGE OF STORMS REACHING GIVEN LATITUDES USING FOUR YEARS (2013–2016) OF BEST-TRACK DATA OF NUMBERED TROPICAL CYCLONES OF ALL AFFECTED OCEAN BASINS

North Atlantic basin (AL) — Total number of storms: 96					
Reached latitude	30° N	35° N	40° N	45° N	50° N
Number of storms	41	29	14	5	2
Percentage	42.7%	30.2%	14.6%	5.2%	2.1%
East North Pacific basin (EP) — Total number of storms: 123					
Reached latitude	30° N	35° N	40° N	45° N	50° N
Number of storms	7	1	0	0	0
Percentage	5.7%	0.8%	0.0%	0.0%	0.0%
West North Pacific basin (WP) — Total number of storms: 166					
Reached latitude	30° N	35° N	40° N	45° N	50° N
Number of storms	51	35	16	4	0
Percentage	30.7%	21.1%	9.6%	2.4%	0.0%
Central North Pacific basin (CP) — Total number of storms: 42					
Reached latitude	30° N	35° N	40° N	45° N	50° N
Number of storms	3	2	1	0	0
Percentage	7.1%	4.8%	2.4%	0.0%	0.0%
North Indian Ocean (IO) — Total number of storms: 65					
Reached latitude	30° N	35° N	40° N	45° N	50° N
Number of storms	0	0	0	0	0
Percentage	0.0%	0.0%	0.0%	0.0%	0.0%
Southern Hemisphere (SH) — Total number of storms: 160					
Reached latitude	30° S	35° S	40° S	45° S	50° S
Number of storms	30	10	0	0	0
Percentage	18.8%	6.3%	0.0%	0.0%	0.0%
Global (2013–2016) — Total number of storms: 652					
Reached latitude	30° N/S	35° N/S	40° N/S	45° N/S	50° N/S
Number of storms	132	77	31	9	2
Percentage	20.2%	11.8%	4.8%	1.4%	0.3%

However, it is questionable whether this is the best way of engineering a single end tile (the northern polar tile in this example) to have enhanced horizontal resolution in a geographical region of interest. If the aim is to furnish a grid with enhanced resolution for a geographical focus area of interest (to which we would rotate the grid to relocate the 'pole' at the center of this region), then we might prefer to have the grid in that end tile to retain the gnomonic cube's property of possessing an equiangular distribution of grid lines in both directions. This would mean sacrificing the property of equiangular (rotated) 'longitudes' of the side tiles, but since their role in this kind of application would be to provide peripheral support to the tile of interest, the price would presumably be acceptable. Although the development of a family of alternative stretched gnomonic grids of this kind is beyond the scope of the present note, it is worth noting that a similar tensioned spline technique (possibly with 'negative tension' in some of the more extreme examples of stretching) can also be employed to formulate them. A future note may discuss this alternative formulation in more detail.

4. Concluding discussion

We have shown how some of the essential properties of the gnomonic cubic grid can be preserved in a fairly simple generalization, from cube to prolate square prism, in such a way that the awkward corners of the grid can be placed slightly closer to the poles. It is important to emphasize that the geometrical adjustment to the grid proposed here does not remove the need to address the challenging technical problem of handling a general moveable nest crossing the corners, since this will still happen occasionally even with corners displaced poleward. However, the proposed adjustment implies a dramatic decrease in the expected *frequency* of the instances where tropical cyclones (and their dedicated nests) need to interact directly with these corner regions of the parent global grid. Thus, from a cosmetic standpoint, the unsightly deformations of the hurricane nests as they traverse these corner regions will at least be seen much less often. The downsides of adopting the proposed adjustment are as follows: the polar tiles will have a slightly higher (and less uniform) resolution than before; this will impose a slightly more restrictive time step condition; the meridional resolution in the side tile must also gradually change with latitude; and the exact three-fold symmetry of the cube's corner configuration is broken.

Another family of modifications that could serve to provide a modestly enhanced resolution to a single end-tile (but not its opposite) is also possible, although we have not examined it in detail here. It would preserve the exact equiangular property of the grid on the selected high-resolution tile, but now at the expense of the equiangular arrangement of what, in an unrotated configuration, would be the longitude lines of the side tile grid. Nevertheless, this alternative family of modifications could be a better candidate than the conformal Schmidt (1977) (or 'Mobius') transformations, especially since the conformal property of the latter is not so valued in a grid framework that is, in any case, of the nonorthogonal kind. The preservation of equiangular great-circle grid line families in the 'focus' tile would then be an attractive property that would greatly simplify the task of introducing further nests there. It is intended to discuss this alternative option in a future note.

Acknowledgments

We are grateful to Tom Black for stimulating discussions and for encouraging this study, and to Mark Iredell and Dusan Jovic who also provided valuable internal reviews.

References

Harris, L. M., and S.-J. Lin 2013 A two-way nested global-regional dynamical core on the cubed-sphere grid. *Mon. Wea. Rev.,* **141,** 283–306.

Lin, S.-J. 2004 A "vertically Lagrangian" finite-volume dynamical core for global models. *Mon. Wea. Rev.,* **132,** 2293–2307.

Lin, S.-J., and R. B. Rood 1996 Multidimensional flux-form semi-Lagrangian transport schemes. *Mon. Wea. Rev.,* **124,** 2046–2070.

McGregor, J. L. 1996 Semi-Lagrangian advection on conformal-cubic grids. *Mon. Wea. Rev.,* **124,** 1311–1322.

McGregor, J. L. 1997 Semi-Lagrangian advection on a cubic gnomonic projection of the sphere. *Atmos. Ocean.,* **35,** 153–169.

Putman, W. M., and S.-J. Lin 2007 Finite-volume transport on various cubed-sphere grids. *J. Comput. Phys.,* **227,** 55–78.

Rančić, M., R. J. Purser, and F. Mesinger 1996 A global shallow-water model using an expanded spherical cube: Gnomonic versus conformal coordinates. *Quart. J. Roy. Meteor. Soc.,* **122,** 959–982.

Ronchi, C., Iacono, R. and Paolucci, P. S. 1996 The 'cubed sphere': A new method for the solution of partial differential equations in spherical geometry. *J. Comput. Phys.,* **124,** 93–114.

Sadourny, R. 1972 Conservative finite-differencing approximations of the primitive equations on quasi-uniform spherical grids. *Mon. Wea. Rev.,* **100,** 136–144.

Schmidt, F. 1977 Variable fine mesh in spectral global models. *Contrib. Atmos. Phys.,* **50,** 211–217.

Schweikert, D. G. 1966 An interpolation curve using a spline in tension. *J. Math. Phys.,* **45,** 312–317.